Journal of Experimental Nanoscience

Publication details, including instructions for authors and subscription information:
http://www.informaworld.com/smpp/title~content=t716100757

Novel 3,4-disubstituted thiophenes for weak passivation of Au nanoparticles

P. Iqbal[a]; K. Critchley[b]; S. Begum[a]; D. Attwood[c]; S. D. Evans[b]; I. P. Jones[d]; J. A. Preece[a]

[a] School of Chemistry, University of Birmingham, Edgbaston, Birmingham B15 2TT, UK [b] Department of Physics and Astronomy, University of Leeds, Leeds LS2 9JT, UK [c] BAE SYSTEMS, Bristol, BS99 7AR, UK [d] School of Metallurgy and Materials, University of Birmingham, Edgbaston, Birmingham B15 2TT, UK

To cite this Article Iqbal, P. , Critchley, K. , Begum, S. , Attwood, D. , Evans, S. D. , Jones, I. P. and Preece, J. A.(2006) 'Novel 3,4-disubstituted thiophenes for weak passivation of Au nanoparticles', Journal of Experimental Nanoscience, 1: 2, 143 — 164

To link to this Article: DOI: 10.1080/17458080500504058

URL: http://dx.doi.org/10.1080/17458080500504058

Journal of Experimental Nanoscience,
Vol. 1, No. 2, June 2006, 143–164

Taylor & Francis
Taylor & Francis Group

Novel 3,4-disubstituted thiophenes for weak passivation of Au nanoparticles

P. IQBAL†, K. CRITCHLEY‡, S. BEGUM†, D. ATTWOOD§,
S. D. EVANS‡, I. P. JONES¶ and J. A. PREECE*†

†School of Chemistry, University of Birmingham,
Edgbaston, Birmingham B15 2TT, UK
‡Department of Physics and Astronomy, University of Leeds,
Leeds LS2 9JT, UK
§BAE SYSTEMS, New Filton House, Filton, Bristol, BS99 7AR, UK
¶School of Metallurgy and Materials, University of Birmingham,
Edgbaston, Birmingham B15 2TT, UK

(*Received October 2005; in final form December 2005*)

Novel self-assembled monolayers of 3,4-disubstituted thiophenes (3,4-dioctylthiophene and 3,4-diheptyloxythiophene) were prepared and characterized by contact angle measurements, ellipsometry and X-ray photoelectron spectroscopy. In addition, Au nanoparticles passivated with the 3,4-disubstituted thiophenes (3,4-dioctylthiophene and 3,4-diheptyloxythiophene) and monosubstituted thiophene (3-octylthiophene) were synthesized and characterized by UV/visible spectroscopy, transmission electron microscopy and dynamic light scattering. The Au nanoparticles had diameters in the range 5–7 nm. The Au nanoparticles stabilized with the thiophene derivatives were, as expected, less stable than the Au nanoparticles passivated with decanethiol and didecylsulfide. Surprisingly, the particles passivated with the monosubstituted 3-octylthiophene were more stable than the 3,4-dioctyl and 3,4-diheptyloxythiophene passivated particles. Such lower stability Au nanoparticles may find uses as negative tone resists in the formation of nanowires by e-beam lithography, via the more readily cleavable Au–S bond

Keywords: Thiophene; SAMs; Au nanoparticles; TEM; XPS

1. Introduction

Self-assembled monolayers (SAMs) provide a versatile approach for derivatizing surfaces such as metals (Au [1] and Ag [1, 2]), semiconductors (Si [3]) and insulators (SiO_2 [4]) with an organic ultrathin film in a controllable, facile and cheap manner. These ultrathin films have attracted immense interest as these SAMs have a wide range of potential applications, ranging from chemically modifying surface properties such as wettability [5], corrosion protection [5, 6] and friction [6], to chemical sensing [7, 8].

More recently it has been demonstrated that SAMs can be chemically modified by direct-writing with an electron beam [9] and photopatterning with X-rays [10].

*Corresponding author. Email: j.a.preece@bham.ac.uk

Journal of Experimental Nanoscience
ISSN 1745-8080 print/ISSN 1745-8099 online © 2006 Taylor & Francis
http://www.tandf.co.uk/journals
DOI: 10.1080/17458080500504058

Subsequently, chemical reactions can be performed on the modified or unmodified regions. The chemical manipulation of such organic surfaces has led to potential application for SAMs to be used for fabrication of electronic components [11].

SAMs on gold surfaces are the most studied and are formed from organosulfur compounds, such as alkylthiols (RSH, **1**) [12–14], dialkyl disulfides (RSSR) [15, 16], dialkyl sulfides (RSR, **2**) [15–17] and more recently thiophene (**3**) [18, 19] and thiophene derivatives (**5** and **6**) [20]. The nature of the Au–S bonding is thought to be a divalent sulfur species for alkylthiols and dialkyl disulfides, where the S–H and S–S bonds are cleaved, respectively, as they chemisorb onto the surface as thiolates [21–23]. In contrast, dialkyl sulfides [17] and thiophene [18] are thought to bond via the sulfur atom directly to the gold surface, such that no bonds are broken, resulting in a trivalent sulfur atom. The strength of the Au–S bond in SAMs formed on gold from alkylthiols or dialkyl disulfides is $126\,\mathrm{kJ\,mol^{-1}}$ [24], for dialkyl sulfides is $60\,\mathrm{kJ\,mol^{-1}}$ [24], and empirical evidence suggest that the sulfur thiophene–gold interaction is weaker [25]. Interestingly earlier X-ray photoelectron spectroscopy (XPS) studies [26] and theoretical calculations [27] suggested that thiophene would not chemisorb onto Au surfaces. The interest in fabricating thiophene SAMs is a result of the electronic properties of polythiophenes [28], as well as their potential applications in optoelectronics and electronic devices, which include field-effect transistors [29] and light transistors [30].

Matsuura *et al*. [18] demonstrated through FTIR-RAS measurements and Langmuir adsorption isotherms that the thiophene SAM growth goes through two stages. At submonolayer coverage the π-faces adsorb to the gold surface. At close to full monolayer coverage, the co-facial π–π interactions between the thiophene molecules dominate over the π–Au surface interaction, and as a result the thiophene bonds solely through the sulfur atom to the Au surface. The thiophene rings are tilted 18° to the normal [19]. The formation kinetics for the monolayer are much slower than for alkylthiols or dialkyl sulfides. Noh *et al*. [20] investigated the relative Au SAM formation adsorption kinetics of octanethiol and 3-octylthiophene. Through surface plasmon resonance studies and STM, it was revealed that the octanethiol SAM formed in 1 hour immersed in a 1 mM solution, whilst the 3-octylthiophene took 4 hours to form in a 1 mM solution. The difference in the SAM formation kinetics between 3-octylthiophene and octanethiol was attributed to two factors [20]. Firstly, the relatively lower affinity of the thiophene molecules to the gold surface. Secondly, a kinetic barrier has to be overcome to break the π–Au interaction as the molecules reorient as the monolayer approaches full coverage. Additionally, it was found that thiophene took longer than 15 hours to form a fully formed SAM [18, 19], suggesting that favourable lateral van der Waals interactions were brought into play by the alkyl chain in 3-octylthiophene which required 4 hours to form a SAM. STM studies revealed thiophene SAMs formed well ordered and closed packed monolayers [18, 19]. Overall, the arrangement of the thiophene SAM is determined by the interactions between sulfur headgroups at the thiophene–Au surfaces and co-facial interactions between thiophene molecules in the self-assembly process.

Alkylthiols [31] have been used as passivants to stabilize colloidal Au nanoparticles. More recently, we [32], and others, [33] have utilized dialkyl sulfides for the passivation of gold nanoparticles. Our motivation for utilizing this weaker coordinating dialkyl sulfide ligand in the stabilization of the Au nanoparticles was to make a material that

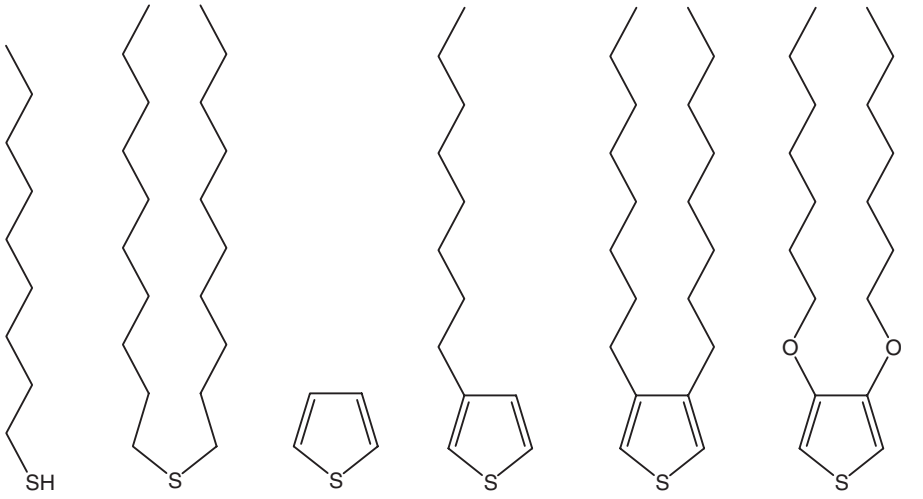

Figure 1. Molecular structures of the ligands used to passivate Au nanoparticles.

would have a cleaner response to a direct-write e-beam lithographic process. It has been demonstrated with alkylthiol SAMs on a Au(III) surface, electron beam irradiation led mostly to cleavage of C–H and C–C bonds of the alkylthiol and ~60% of the original Au–thiolate bonds remained [34]. Thus, residual carbon and sulfur contamination seems inevitable in direct-write e-beam lithography with alkylthiol passivated Au nanoparticles, which will affect the conductivity of the gold nanostructures.

We reasoned that the use of dialkyl sulfides as a passivant for gold nanoparticles would lead to a cleaner gold material after direct-writing with an e-beam. The much weaker Au–S bond would be cleaved at a relatively faster rate than the hydrocarbon bonds allowing the dialkyl sulfide to vaporize into the UHV e-beam writing chamber. We did in fact find this was the case, but there was still some carbon contamination in the gold [35].

Therefore, we are now extending our design criteria even further by introducing an even weaker ligand to passivate gold nanoparticles, based on thiophene. Thus, in this paper we detail for the first time the synthesis of Au nanoparticles passivated with novel thiophene derivatives (figure 1), as well as the SAM formation of these novel thiophene derivatives on Au surfaces.

2. Experimental

2.1. *Chemicals*

Chemicals were purchased from Aldrich except for thiophene (Acros Organics) and 3-bromothiophene and didecylsulfide (Lancaster). Didecyl sufide was further purified after purchase by recrystallization from EtOH and dried in high vacuum for 2 days. Anhydrous quinoline was dried over zinc powder under N_2 atmosphere and collected

under vacuum (55°C, 0.1 mbar) Thin-layer chromatography (TLC) was carried out on aluminium plates coated with silica gel 60 F254 (Merck 5554). The TLC plates were air-dried and analysed under a short-wave UV lamp (254 nm). Column chromatographic separations were performed on silica gel 120 (ICN Chrom 32-63, 60 Å).

2.2. *NMR*

^{1}H nuclear magnetic resonance (NMR) spectra were recorded on a Bruker AC 300 (300.13 MHz) spectrometer. ^{13}C NMR spectra were recorded on a Bruker AV 300 (75.5 MHz) using Pendent pulse sequences. All chemical shifts are quoted in ppm to higher frequency from Me_4Si using either deuterated chloroform ($CDCl_3$) or methanol (CD_3OD) as the lock and the residual solvent as the internal standard. The coupling constants are expressed in hertz (Hz) with multiplicities abbreviated as follows; s = singlet, d = doublet, dd = double doublet, t = triplet, q = quartet and m = multiplet.

2.3. *Mass spectroscopy (MS)*

Electron impact mass spectroscopy (EIMS) was performed on VG Prospec and electrospray mass spectroscopy (ESMS) was performed on a Micromass time of flight (TOF) instrument using methanol as the running solvent.

2.4. *Infrared spectroscopy (IR)*

The IR spectra were recorded as thin solid films on NaCl disks using a Perkin Elmer 1600 FT-IR.

2.5. *Elemental analysis*

Elemental analysis was carried out on a Carlo Erba EA 1110 (C H N) instrument.

2.6. *High-performance liquid chromatograph*

High-performance liquid chromatography (HPLC) were recorded on a Dionex Summit System with Chromeleon Software, with a Summit UVD 170s UV/visible multichannel detector with analytical flow cell. Analytical HPLC runs were performed on a Luna (Phenomenex), C_{18}, 250 mm × 4.6 mm ID, with 10 μm pore size column using a gradient of MeCN/H_2O 50/50 over 60 min.

2.7. *3,4-dioctylthiophene (5)* [36]

A solution of octylmagnesium bromide (5.40 g, 24.90 mmol) was added dropwise to a solution of 3,4-dibromothiophene (**7**) (2.00 g, 8.30 mmol) and [1,3-bis(diphenylphosphino)propane]nickel (II) chloride (0.03 g) as catalyst in dry THF (15 ml) under N_2 atmosphere at 0°C. The reaction mixture was gently heated at 50°C for 16 hours. The reaction mixture was cooled to room temperature, and water (25 ml) containing a few drops of conc. HCl was added dropwise to the reaction mixture whilst cooling with

an ice bath maintaining the temperature at 20°C. The resulting precipitate was removed by filtration and the filtrate was extracted with Et_2O (3 × 50 ml). The combined extracts were washed with brine (25 ml), dried ($MgSO_4$), filtered, and the filtrate was concentrated *in vacuo*, affording the crude product which was purified via HPLC to yield a colourless oil (1.51 g, 59%), retention time = 28.80 min. ^{1}H NMR (300 MHz, $CDCl_3$): 6.88 (s, 2H, Tp–H), 2.49 (t, $J = 7.91$ Hz, 4H, $C\underline{H}_2C_7H_{15}$), 1.67–1.55 (m, 4H, $CH_2C\underline{H}_2C_6H_{17}$), 1.37–1.28 (m, 20H, $CH_2CH_2C_5\underline{H}_{10}C\underline{H}_3$), 0.88 (t, $J = 6.62$ Hz, 6H, C_7H_{14}–$C\underline{H}_3$); ^{13}C NMR (75 MHz, $CDCl_3$): δ_C 141.5, 119.3, 31.3, 29.1, 29.1, 28.9, 28.7, 28.2, 22.1, 13.5; ν_{max}/cm^{-1} (nujol); m/z (EIMS): 331 ($[M + Na]^+$, 100%); elemental analysis for $C_{20}H_{36}S$ reqiures C 77.85%, H 11.76% found C 77.75%, H 11.86%.

2.8. *Synthesis of 3,4-diheptyloxythiophene* [28]

2.8.1. Diethyl thiodiglycolate (9). To a solution of thiodiglycolic acid (**8**) (20.00 g, 133.20 mmol) in EtOH (100 ml), conc. H_2SO_4 (8 ml) was added dropwise and heated under reflux for 24 hours with a $CaCl_2$ guard. The reaction mixture was allowed to cool to room temperature and concentrated *in vacuo* (50 ml). H_2O (100 ml) was added and the aqueous layer extracted with Et_2O (3 × 50 ml). The combined organic layers were further washed with saturated Na_2CO_3 (2 × 30 ml), dried ($MgSO_4$), filtered and concentrated *in vacuo* to afford a colourless oil (21.66 g, 79%). ^{1}H NMR (300 MHz, $CDCl_3$): 4.19 (q, $J = 7.13$ Hz, 4H, $OC\underline{H}_2CH_3$), 3.37 (s, 4H, $SC\underline{H}_2$), 1.28 (t, $J = 7.13$ Hz, 6H, $OCH_2C\underline{H}_3$); ^{13}C NMR (75 MHz, $CDCl_3$): δ_C 160.0, 61.2, 33.6, 13.8; ν_{max}/cm^{-1} (film): 1736; m/z (EIMS): 206 ($[M]^+$, 35%), 160 ($[M - 2 \times (C_2H_4)]^+$, 100%).

2.8.2. Diethyl 3,4-dihydroxythiophene-2,5-dicarboxylate (10). A solution of **9** (5.00 g, 24.27 mmol) and diethyl oxalate (8.90 ml, 65.61 mmol) in EtOH (20 ml) was added dropwise into an ice cooled solution of NaOEt (0°C) (7.43 g, 109.26 mmol) in EtOH (80 ml). The reaction mixture was heated under reflux for 1 hour. The resulting yellow precipitate was washed thoroughly with EtOH (100 ml). The precipitate was dissolved in H_2O (200 ml) and acidified with HCl (1 M). The resulting precipitate was collected through filtration, washed thoroughly with H_2O (50 ml) and dried in air, affording a white solid (4.50 g, 71%). mp: 124–126°C; ^{1}H NMR (300 MHz, $CDCl_3$): 9.39 (s, 2H, OH), 4.39 (q, $J = 7.13$ Hz, 4H, $OC\underline{H}_2CH_3$), 1.38 (t, $J = 7.13$ Hz, 6H, $OCH_2C\underline{H}_3$); ^{13}C NMR (75 MHz, $CDCl_3$): δ_C 160.7, 150.4, 104.6, 60.4, 12.8; ν_{max}/cm^{-1} (nujol): 3325, 1688, m/z (ESMS): 283 ($[M + Na]^+$, 100%).

2.8.3. Diethyl 3,4-diheptyloxythiophene-2,5-dicarboxylate (11). A suspension of K_2CO_3 (0.66 g, 4.81 mmol) in a solution of **10** (1.50 g, 5.77 mmol), 1-bromoheptane (4.13 g, 23.06 mmol) in DMF (100 ml) was heated under reflux for 20 hours. The reaction mixture was allowed to cool to room temperature and concentrated *in vacuo* (30 ml). H_2O (50 ml) was added and the aqueous layer was extracted with Et_2O (3 × 50 ml). The combined organic layers were washed with brine (30 ml), dried ($MgSO_4$), filtered and the filtrate concentrated *in vacuo*, yielding an orange oil as the crude product. The crude product was purified via silica gel column chromatography (graded elution: 0 to 15% EtOAc in hexane, increments of 5% per 100 ml of

eluent used). The solvent was removed *in vacuo* to yield pale yellow oil (2.10 g, 80%). ^{1}H NMR (300 MHz, $CDCl_3$): 4.33 (q, $J = 7.13$ Hz, 4H, $OC\underline{H}_2CH_3$), 4.13 (t, $J = 6.62$ Hz, 4H $O–C\underline{H}_2C_6H_{12}$), 1.80–1.72 (m, 4H, $OCH_2C\underline{H}_2C_5H_{11}$), 1.56–1.28 (m, 16H, $OC_2H_4(C\underline{H}_2)_4CH_3$), 1.36 (t, $J = 7.13$ Hz, 6H, $OCH_2C\underline{H}_3$), 0.87 (t, $J = 6.62$ Hz, 6H, $OC_6H_{12}C\underline{H}_3$); ^{13}C NMR (75 MHz, $CDCl_3$): δ_C 160.5, 153.3, 117.4, 74.9, 61.1, 31.6, 29.9, 28.9, 25.6, 22.4, 14.0, 13.8; ν_{max}/cm^{-1} (film): 1720, 1550; m/z (ESMS): 479 ($[M + Na]^+$, 100%).

2.8.4. Diethyl 3,4-diheptyloxythiophene-2,5-dicarboxylic acid (12). An aqueous solution (5 ml) of sodium hydroxide (0.63 g, 15.79 mmol) was added to a solution of **11** (1.80 g, 3.95 mmol) in MeOH (50 ml). The reaction mixture was heated under reflux for 20 hours. The resultant colourless solution was allowed to cool to room temperature and concentrated *in vacuo* (~20 ml). H_2O (50 ml) was added and acidified with conc. HCl. The resulting white precipitate was filtered and air-dried to afford a white solid (1.42 g, 90%). mp: 165–167 °C; ^{1}H NMR (300 MHz, CD_3OD): 4.14 (t, $J =$ 6.44 Hz, 4H, $OC\underline{H}_2C_6H_{13}$), 1.79–1.70 (m, 4H, $OCH_2C\underline{H}_2C_5H_{11}$), 1.49–1.32 (m, 16H, $OC_2H_4(C\underline{H}_2)_4CH_3$), 0.90 (t, $J = 6.99$ Hz, 6H, $OC_6H_{12}C\underline{H}_3$); ^{13}C NMR (75 MHz, $CDCl_3$): δ_C 163.3, 155.7, 121.4, 78.0, 35.0, 33.2, 32.2, 28.9, 25.7, 16.4; ν_{max}/cm^{-1} (nujol): 1674, 1545; m/z (ESMS): 423 ($[M + Na]^+$, 100%).

2.8.5. 3,4-diheptyloxythiophene (6). A suspension of copper chromite (0.31 g, 1.00 mmol) in a solution of **12** (4.00 g, 10.00 mmol) in anhydrous quinoline (25 ml) was heated at 160°C under N_2 atmosphere for 3 hours. The mixture reaction was allowed to cool to room temperature and Et_2O (50 ml) was added. The resulting black solid was removed by filtration. The filtrate was washed with 5% HCl (3×25 ml) and saturated NaCl (2×25 ml). The organic extract was dried ($MgSO_4$), filtered and the filtrate concentrated in *vacuo*. The crude product was purified via silica gel column chromatography (graded elution: 0 to 10% EtOAc in hexane, increments of 5% per 100 ml of eluent used). The solvent was removed in *vacuo* to yield a white solid (2.53 g, 81%). Mp: 178–180°C; ^{1}H NMR (300 MHz, $CDCl_3$): 6.15 (s, 2H, Tp–H), 3.96 (t, $J = 6.75$ Hz, 4H, $OC\underline{H}_2C_6H_{13}$), 1.85–1.76 (m, 4H, $OCH_2C\underline{H}_2C_5H_{11}$), 1.45–1.29 (m, 16H, $OC_2H_4(C\underline{H}_2)_4CH_3$), 0.88 (t, $J = 6.75$ Hz, 6H, $OC_6H_{12}C\underline{H}_3$); ^{13}C NMR (75 MHz, $CDCl_3$): δ_C 148.1, 96.9, 70.7, 31.9, 29.1, 26.0, 22.7, 14.2; ν_{max}/cm^{-1} (nujol): 2922, 2855, 1565, 1505; m/z (EIMS): 312 ($[M]^+$, 25%); (HRMS): found: 312.211856, calculated mass: 312.212302, elemental analysis for $C_{22}H_{26}O_2S$ requires C 69.18%, H 10.34% found C 69.29%, H 10.34%.

2.9. *Preparation of gold substrate*

The gold substrates were prepared using an Auto 306 vacuum evaporation chamber (Edwards) on glass microscope slides (BDH). Prior to the evaporation of gold onto the glass slides, a Cr layer (6 nm) was evaporated onto the glass slides to promote adhesion of the gold to the base material. Cr was deposited by heating Cr pieces by electrical resistance using a voltage of 30 V and a current of 3 A. Au was deposited via heating a gold wire placed into a Mo boat held within the auto 306 vacuum evaporation chamber,

using a two-pump system, and the pressure was reduced to $\sim 10^{-4}$ bar followed by a subsequent reduction to $\sim 10^{-7}$ bar. Deposition and deposition rate were monitored using a quartz crystal microbalance (QCM) thickness monitor. The deposition rate used for both Cr and Au was in the range of 0.05–0.10 nm^{-1}.

2.10. *Preparation of SAMs*

Prior to the preparation of the SAMs the glassware and the gold substrates were cleaned thoroughly to remove contaminants. Initially, the glassware was washed thoroughly with piranha solution (conc. H_2SO_4: 30% $H_2O_2 = 7:3$) followed by rinsing with Ultra-High Pure (UHP) H_2O. The subsequent steps were followed: 30 min sonication in UHP H_2O, dried in an oven at 120°C for 30 min, allowed to cool to room temperature, 30 min sonication in EtOH, dried in an oven at 120°C for 30 min and wrapped in aluminium foil before use to prevent exposure to airborne contaminates and used within 24 hours. The gold substrates were immersed in piranha solution at room temperature for 10 min with occasional stirring, followed by thorough rinsing with UHP H_2O, then with EtOH (HPLC grade) and immediately immersed in the desired 1 mM solution of **1–6** for 24 hours. Finally, the SAMs were rinsed thoroughly with EtOH (HPLC grade) and dried with a stream of N_2.

2.11. *Ellipsometry*

The thickness of the deposited monolayers was determined by spectroscopic ellipsometry. A Jobin-Yvon UVISEL ellipsometer with a xenon light source was used for the measurements. The angle of incidence was fixed at 70°. A wavelength range of 280–820 nm was used. The DeltaPsi software was employed to determine the thickness values and the calculations were based on a three-phase ambient/SAM/Au model, in which the SAM was assumed to be isotropic and assigned a refractive index of 1.50. The thickness reported is the average of six measurements taken on each SAM.

2.12. *Water contact angle*

Contact angles were determined by the sessile drop method using a home built contact angle apparatus, equipped with a charged coupled device (CCD) camera that is attached to a personal computer for video capture. To measure advancing (θ_a) or receding (θ_r) contact angles, the angle was measured as a micro-syringe was used to quasi-statically add liquid to or remove liquid from the drop. The drop is shown as a live video image on the PC screen and digitally recorded for future analysis of the images. The acquisition rate was four frames per second. Stored images of the droplet were analysed by using software from FTÅ. Contact angles were determined from an average of five different measurements on each sample.

2.13. *X-ray photoelectron spectroscopy (XPS)*

XPS spectra were obtained on an ESCALAB 250 controlled by an Avantage data system. XPS experiments were carried out using a monochromatic Al K_α X-ray source

(1486.6 eV) operated at 15 kV and 150 W. The pressure in the analysis chamber was in the range 10^{-9}–10^{-10} mbar. Survey spectra were obtained using a pass energy of 150 eV and a step size of 1 eV. Si (2p), C (1s), O (1s), N (1s), Au (4f) and Ag (3d) spectra were recorded using a pass energy of 20 eV and a step size of 0.10 eV. In order to minimize charge retention on the sample, the samples were clipped onto the holder using stainless steel or Cu clips.

2.14. *General procedure for the synthesis of Au nanoparticles passivated with 1–6*

The Au-particles stabilized with **1–6** were prepared using the two-phase method demonstrated by Brust *et al.* [31] A solution of tetraoctylammonium bromide (1.12 mmol) in PhMe (30 ml) was added to a vigorously stirred solution of $HAuCl_4 \cdot 3H_2O$ (0.51 mmol) in UHQ H_2O (30 ml). Upon addition the organic phase changes colour from colourless to red/orange. After 45 min of vigorous stirring the organic phase was separated from the aqueous layer. A solution of **1–6** (0.51 mmol) in PhMe (30 ml) was added to the organic phase, followed by dropwise addition of $NaBH_4$ in UHQ H_2O (30 ml). Upon addition of the aqueous $NaBH_4$ the colour of the organic phase changed from reddish orange to dark red/purple (in case of **1** to brown). The two-phase mixture was stirred vigorously for 3 hours. The organic phase was separated from the aqueous phase. In the case for **1** and **3–6**, the colloidal solutions were concentrated down to 10 ml *in vacuo* at 35–40°C. The particles were purified by precipitation from the PhMe with MeCN followed by centrifugation of the suspension. The supernatant was discarded and the precipitate redissolved in $CHCl_3$ (1 ml). The precipitation was repeated twice for Au nanoparticles passivated with **1** and **2**. However, for nanoparticles stabilized with **3–6** the precipitation procedure for purification was carried out once due to the lower stability of the particles to this process.

2.15. *Synthesis of the TOAB Au nanoparticles*

The general procedure followed was the same as for synthesis of the Au nanoparticles stabilized with **1–6**; the only modifications made to the procedure were that during reduction of the particles with aqueous solution of $NaBH_4$ no solution of ligand in PhMe was added. Also the TOAB Au nanoparticles were purified through washing with 0.1 M H_2SO_4 (2×15 ml), 1 M Na_2CO_3 (2×15 ml) and with UHQ H_2O (15 ml).

2.16. *UV/visible absorption spectroscopy*

UV/visible spectra were recorded in $CHCl_3$ (1 ml) using a Hewlett-Packard 8452A scanning spectrophotometer equipped with a 1 cm path length quartz cell. The UV/visible study on the particles was carried out starting at a set point absorption of λ_{max} at $\sim$0.7 A. Spectra were taken each hour for 19 hours.

2.17. *Transmission electron microscopy*

Transmission electron microscopy (TEM) images were obtained using a JEOL-JEM 1200 EX electron microscope operating at an accelerating voltage of 80 keV and

spot size 1. The samples were prepared by depositing a dilute (<1 mg ml^{-1}) $CHCl_3$ solution of the nanoparticles onto a carbon coated Cu TEM grid and allowing the solvent to evaporate. Nanoparticle core size distributions were determined by the measurement of 150–250 particles.

2.18. *Dynamic light scattering*

Dynamic light scattering (DLS) measurements were performed using a high-performance particle sizer (HPPS) incorporating NIBS^{TM} Technology, Malvern Instruments. The measurements were taken using toluene as solvents.

3. Results and discussion

3.1. *Synthesis of 3,4-dioctylthiophene (5) and 3,4-diheptyloxythiophene (6)*

3,4-dioctylthiophene (**5**) was synthesized from a grignard reaction in the presence of the catalyst [1,3-bis(diphenylphosphino)propane]nickel (II) chloride and octylmagnesium bromide (scheme 1). 3,4-diheptyloxythiophene **6** was attained via an adapted procedure, which has been described by Stephan *et al.* [28] (scheme 2). The synthesis of **9** was attained through an esterification of **8**. Diethyl dioxalate was reacted with **9** through an enol reaction, with NaOEt as the base to yield **10**. **10** was alkylated in basic condition (K_2CO_3), at elevated temperatures of 110–120° in DMF to afford **11**. A basic hydrolysis reaction yielded **12**. Finally, decarboxylation of **12** was achieved in the presence of copper chromite as catalyst at elevated temperature (160°C) in quinoline to yield **6**.

3.2. *Self-assembled monolayers (SAMs)*

3.2.1. Preparation of the SAMs. The SAMs of **1–6** were formed by immersion of the Au substrates in 1 mM solution of **1–6** in EtOH for 24 hours. After the 24 hours the Au substrates were thoroughly rinsed with EtOH (HPLC grade) and dried with a stream of N_2.

3.2.2. X-ray photoelectron spectroscopy (XPS). XPS spectra were recorded for all SAMs formed from **1–6**. The spectra show the presence of all of the elements present in **1–6**, i.e. C, S and O as well as the Au signals from the substrate. Figure 2 is the XPS spectrum of the SAM formed from **5** that reveals the characteristic signatures that

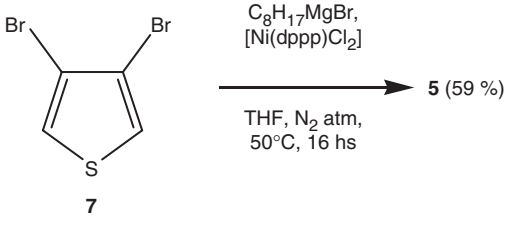

7

Scheme 1. Synthesis of 3,4-dioctylthiophene.

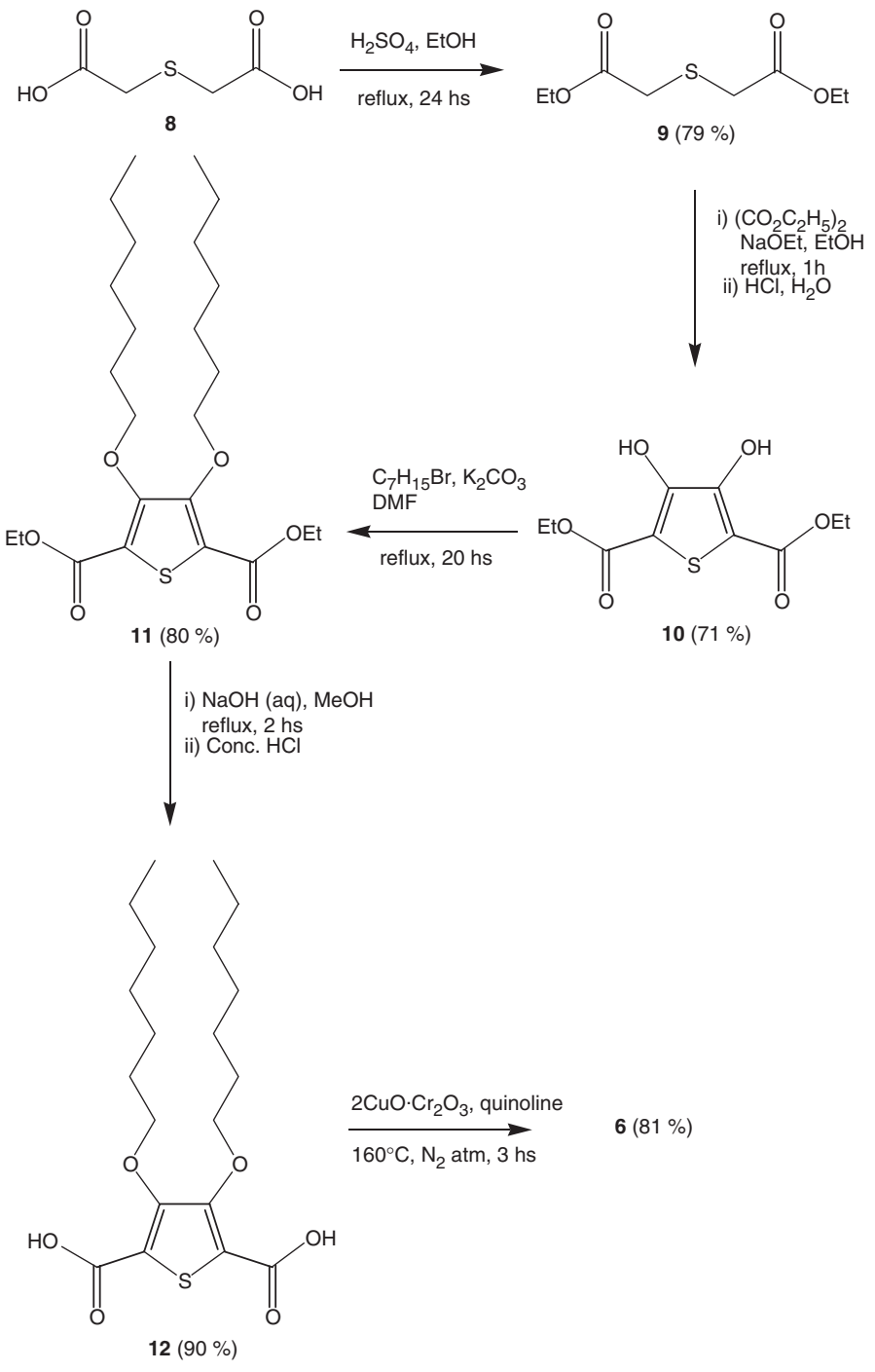

Scheme 2. Synthesis of 3,4-diheptyloxythiophene.

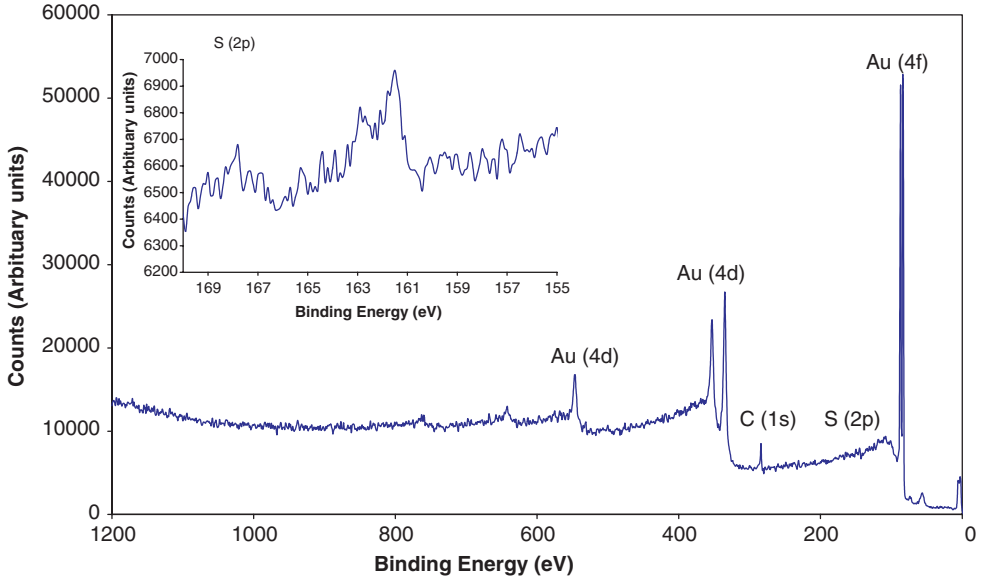

Figure 2. XPS spectra (0–1200 eV and S (2p) region) for SAM formed from **5**.

are expected (XPS spectra of the SAMs formed from **1–4** and **6** are shown in the supplementary information).

3.2.3. Contact angle measurements. Decanethiol (**1**) SAM as expected is very hydrophobic due to the surface exposed alkyl functionality. The advancing contact angle (θ_a) of 114° and receding contact angle of (θ_r) 91° as is didecylsulfide with θ_a of 110° and θ_r of 91°, which are typical for these SAMs [16] (table 1). The thiophene SAMs **3–6** are less hydrophobic having θ_a of ~90°.

3.2.4. SAM thickness. The monolayer thicknesses attained for **1** and **2** of 1.30 ± 0.1 nm and 1.20 ± 0.15 nm, respectively (table 1), compares well with documented values [15]. Furthermore, the SAM formed from **4** (1.24 ± 0.19 nm) has similar thickness as observed by Noh *et al.* [20] through surface plasmon resonance spectroscopy. The SAM formed from **3** has a thickness of 0.20 ± 0.11 nm, which equates to half the thickness of the calculated molecular length, but undoubtedly there is some tilting of the thiophene units to the surface normal. Assuming a densely packed monolayer the tilt angle to the normal of the substrate is 57°. This value is larger than the value quoted by Noh *et al.* (18°) [19].

In the case of the two chain substitutes, **5** and **6**, the thickness values are 0.84 ± 0.14 and 0.86 ± 0.09 nm, respectively, and as such are significantly lower than the single chain derivative **4**. Clearly, there are significant differences in the packing of the monosubstituted and disubstituted thiophene derivatives in the SAM and requires further investigation.

Table 1. SAM characterization by contact angle and ellipsometry.

SAM	θ_a/°	θ_r/°	Experimental thickness/nm	Calculated thickness/nm[a]
Decanethiol (**1**)	114 ± 5	91 ± 5	1.30 ± 0.10	1.39
Didecyl sulfide (**2**)	110 ± 1	91 ± 1	1.20 ± 0.15	1.37
Thiophene (**3**)	83 ± 2	58 ± 2	0.20 ± 0.11	0.36
3-Octylthiophene (**4**)	88 ± 2	60 ± 3	1.24 ± 0.19	1.34
3,4-Dioctylthiophene (**5**)	91 ± 4	68 ± 4	0.84 ± 0.14	1.35
3,4-Diheptyloxythiophene (**6**)	91 ± 2	73 ± 2	0.86 ± 0.09	1.33

[a]The calculated molecular length was determined by Chem3D Ultra version 7.0 software and minimized through MM2; no account for any possible molecular tilt has been introduced.

3.3. *Nanoparticles*

3.3.1. Synthesis of the nanoparticles. The particles were synthesized following the Brust two-phase method [31]. An aqueous Au salt was transferred from the aqueous layer to the organic with the aid of tetraoctylammonium bromide (TOAB) as the phase transfer reagent. The Au salt was reduced by $NaBH_4$ in the presence of the passivant **1–6**, leading to red/purple coloured solutions in the organic phase.

The Au nanoparticles passivated with the thiophene derivatives **4–6** were unstable in comparison to the Au nanoparticles passivated with decanethiol (**1**) and didecyl sulfide (**2**). The particles stabilized with the thiophene derivatives **4–6** could only be precipitated and centrifuged once during purification, as a second precipitation led to aggregation and irreversible precipitation of the gold. The Au nanoparticles stabilized with **4–6**, if left desolvated for more than 1 min, would not redisperse in organic solvents. The stability of the nanoparticles passivated with **4–6** in solution was found to be concentration dependent, similar to didecylsulfide passivated Au nanoparticles [32]. At low concentrations (0.1 mg ml^{-1}) the nanoparticle cores aggregated and precipitated within 1 hour, while in a more concentrated solution (10 mg ml^{-1}) the particles were stable for up to 2 days. More concentrated solutions were examined, but the particles did not show an improvement in stability. These results suggest that the relatively weak Au-thiophene bond leads to an equilibrium in solution being established that favours the unbound thiophene, allowing the Au cores to aggregate. Previously, we had observed a similar phenomenon with didecyl sulfide, where at concentrations of 1 mg ml^{-1} the particles were stable indefinitely [32]. The difference in stability between the thiophene derivatives **3–6** and didecyl sulfide **2** is the result of the stronger Au–sulfide interaction in comparison to the Au–thiophene.

3.3.2. Characterization of the Au nanoparticles

3.3.2.1. *UV/visible spectroscopy*. The UV/visible spectra **1–2** and **4–6** passivated Au nanoparticles (figure 3) reveal the plasmon resonance band at ~520 nm typical for particles with diameters <10 nm [31–33]. The shallow absorption band at ~504 nm for Au nanoparticles stabilized with **1** and strong absorption band with λ_{max} at 520 nm for the Au nanoparticles stabilized with **2** are in accordance with reported UV/visible

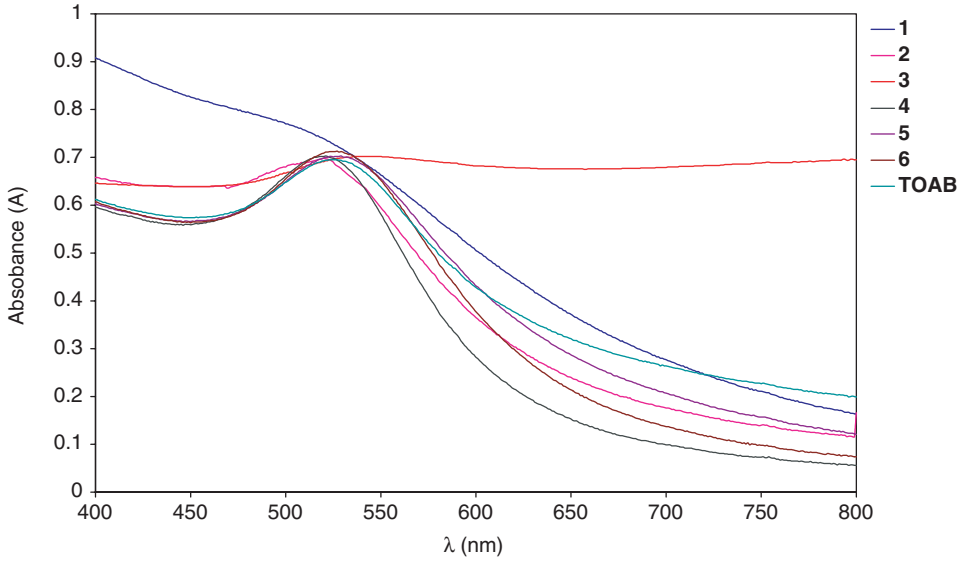

Figure 3. UV spectra of Au nanoparticles passivated with **1**, **2**, **4**, **5**, and **6** in $CHCl_3$ solution.

Table 2. Determination of the sizes of the nanoparticles stabilized with a number of different ligands by various techniques: TEM, dynamic light scattering (DLS) as well as λ_{max} from UV/visible spectroscopy.

Ligand	Plasmon resonance band (λ_{max})/nm	TEM/nm[a]	DLS/nm
Decanethiol (**1**)	504	2.3 ± 0.9	4.00
Didecylsulfide (**2**)	520	5.2 ± 0.8	6.43
Thiophene (**3**)	535	–	–
3-Octylthiophene (**4**)	521	5.9 ± 1.2	8.14
3,4-Dioctylthiophene (**5**)	529	6.1 ± 1.1	8.06
3,4-Diheptyloxythiophene (**6**)	527	6.3 ± 0.9	8.55
TOAB (in toluene)	520	5.6 ± 1.1	7.05

[a]Diameter obtained from between 150 and 250 particles.

absorptions [31–33]. Au nanoparticles stabilized with **3** were unstable and precipitated after 5 min, however, a UV/visible spectrum was taken immediately after purifying once via precipitation from toluene by addition of MeCN. The spectrum was very broad, and λ_{max} was at a higher wavenumber (535 nm). After the UV/visible analysis the solution had turned blue from the original red/purple solution and on the side of the UV cell a black/blue solid was observed, suggesting aggregation and precipitation of the Au nanoparticles.

3.3.2.2. *Dynamic light scattering (DLS).* DLS measurements (table 2) of the Au nanoparticles stabilized with the thiophene derivatives **4–6** indicate that the core diameters are 8.14, 8.06 and 8.55 nm, respectively, and are larger in comparison to the Au nanoparticles passivated with **1**, **2** and TOAB, which are 4.00, 6.43 and 7.06 nm, respectively. The larger core diameters of the thiophene passivated Au particles would

be in line with the weak Au–S interaction, allowing the Au (0) atoms to aggregate for longer before total passivation with the thiophene derivatives **4–6**.

3.3.2.3. *TEM analysis*. TEM measurements (table 2) show that the Au nanoparticles stabilized with **1** and **2** are 2.3 ± 0.9 nm and 5.2 ± 0.8 nm, respectively, and are similar to documented values using a similar procedure for the synthesis of these nanoparticles [32]. The Au particles passivated with the thiophene derivatives **4–6** are larger at 5.9 ± 1.2, 6.1 ± 1.1 and 6.3 ± 0.9 nm (figure 4). Thus, these findings support our initial belief that the weaker thiophene Au–S interaction, in comparison to alkanethiol and dialkyl sulfide, would lead to a slower passivation and therefore increased particle size.

The TEM analysis reveals the diameters are of the order of 25% smaller than those obtained by DLS. The TEM analysis is a direct method of obtaining the diameter and we feel is more reliable.

3.4. *Nanoparticles stability in solution*

Stability of Au nanoparticles passivated with **1** and **2** as previously reported were stable indefinitely at room temperature, but the Au nanoparticles passivated with **2** would aggregate over several hours at 50°C in $CHCl_3$ [32].

A time-dependent UV/visible study over 19 hours at room temperature for the Au nanoparticles stabilized with **4–6** in $CHCl_3$ solution (figure 5) reveal that the particles differ in stability relative to each other and are less stable than particles passivated with **1** and **2**. For Au nanoparticles stabilized with **4**, the UV/visible spectra reveal the particles are stable over the 19 hours (figure 5a).

In the case of the Au nanoparticles stabilized with **5** the λ_{max} as 529 nm (surface plasmon) decreases with time with a concomitant increase in a broad band at ~700 nm (figure 5b). This behaviour is indicative of the original particles aggregating to form larger particles which then precipitate [37]. Also after 19 hours, the Au nanoparticle solution lost its red/purple colour and evolved to a blue solution and black solid was deposited on the side of the UV cell.

Interestingly, Au nanoparticles passivated with **6** have a slightly different time-dependent UV/visible behaviour (figure 5c). In this case, the λ_{max} at 527 nm decreases with time, but there is no concomitant growth of any aggregation band at 700 nm. However, a precipitate was observed in this experiment, as was observed for the Au nanoparticles passivated with **5**. The Au nanoparticle solution after the UV/visible study retained the red/purple colour.

The decrease in the absorption bands at 521, 529, and 527 nm as a function of time for each set of Au nanoparticles passivated with **4**, **5**, **6**, respectively, is shown in figure 6. Clearly nanoparticles passivated with **4** are the most stable and the Au nanoparticles passivated with **6** are more stable than **5**. It is worth noting that the SAM formed from **4** is thicker than those formed from **5** and **6**. Coupling this difference in thickness to the greater stability of the Au nanoparticles passivated with **4**, it seems that the SAM of **4** is relatively more stable. In addition, the replacement of the α-methylene unit in **5** with oxygen to give **6** significantly increased the stability of the Au nanoparticles. Presumably, the π-donation of the oxygen lone pair to the thiophene ring enhances the Au–S interaction with **6**, relative to **5**.

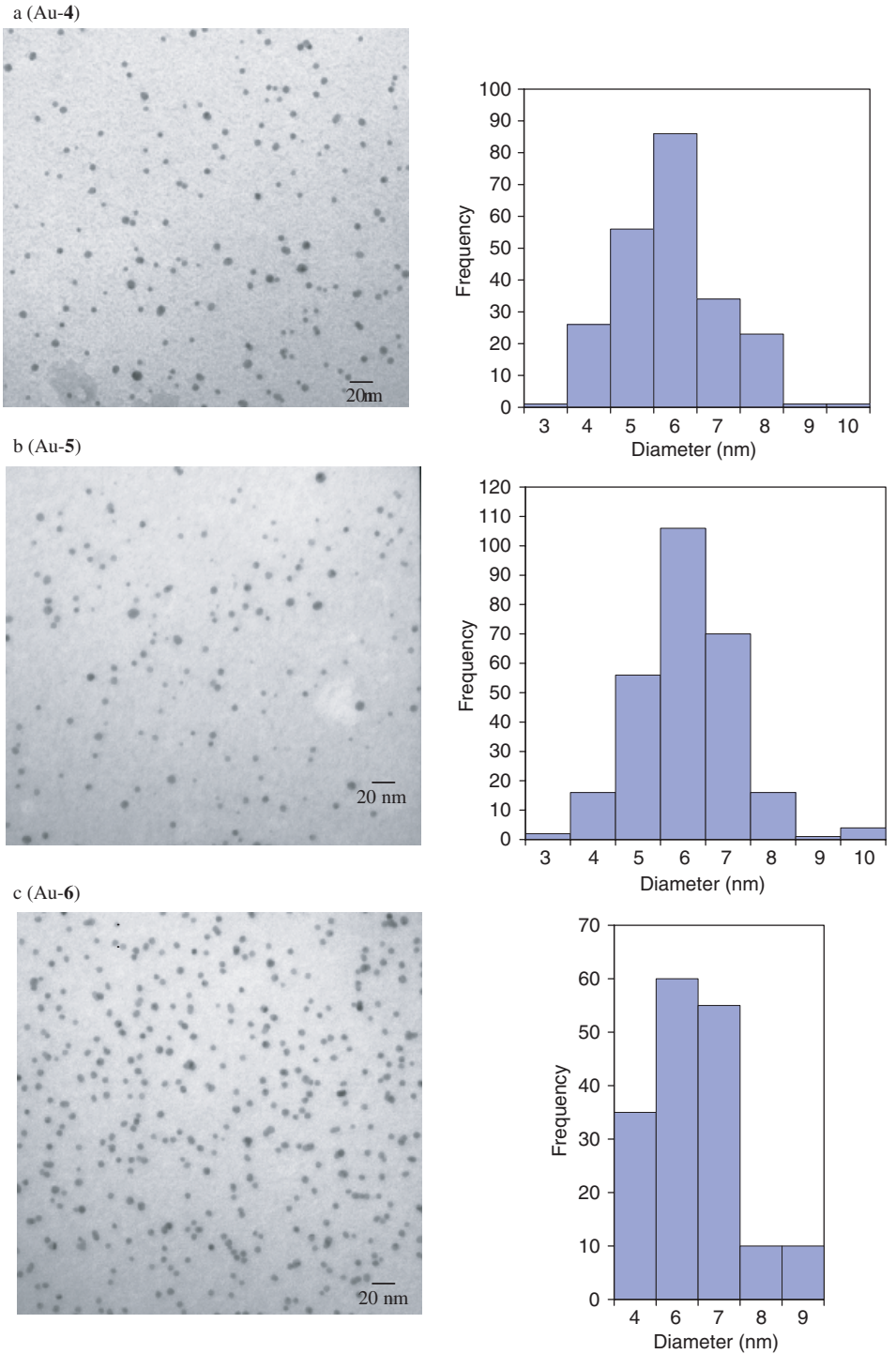

Figure 4. TEM micrographs and size distributions for Au nanoparticles stabilized by (a) **4**, (b) **5**, (c) **6**.

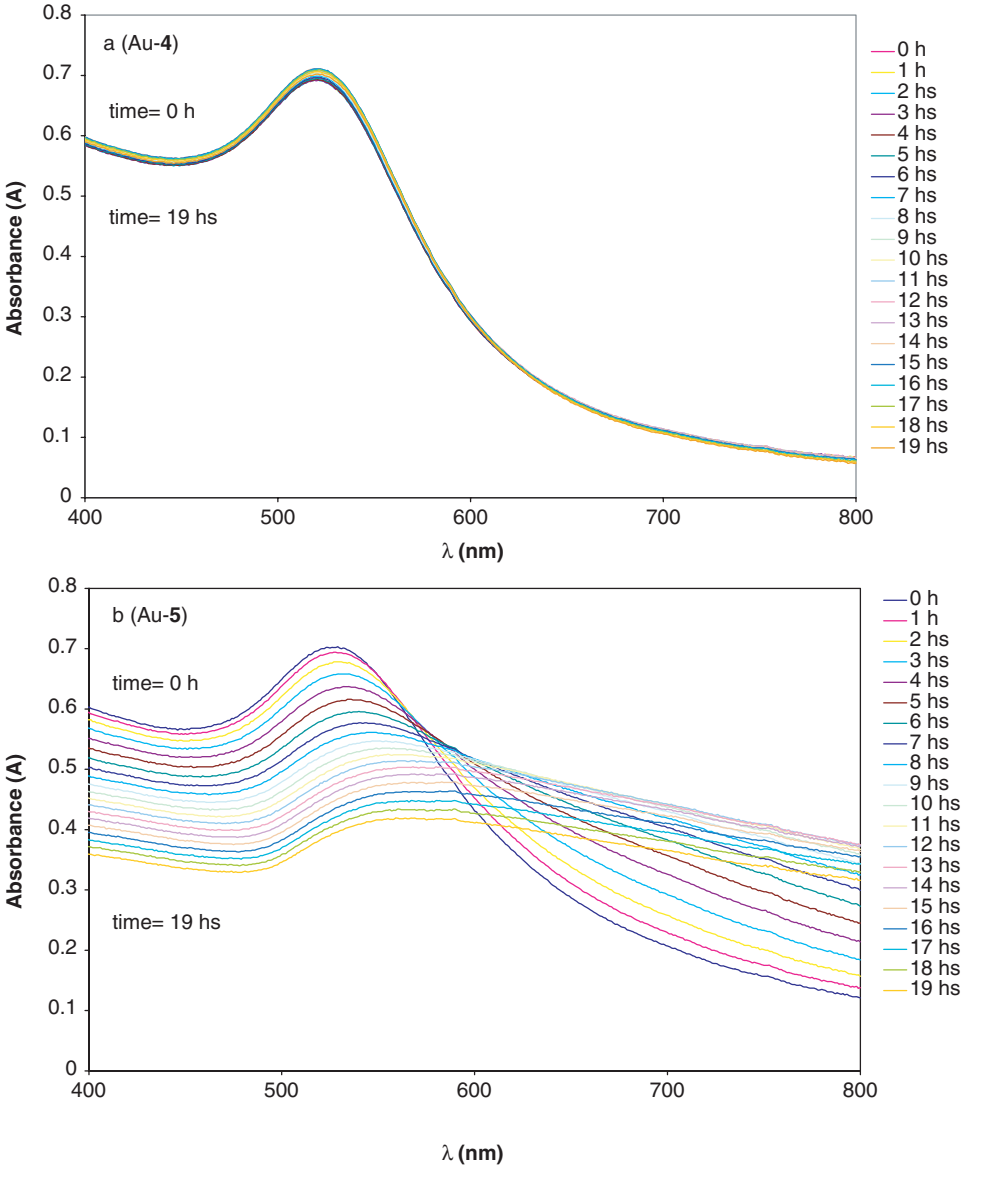

Figure 5. UV/visible spectra recorded hourly over 19 hours for the Au nanoparticles stabilized with (a) **4**, (b) **5** and (c) **6**.

4. Conclusion

SAMs of novel 3,4-disubstituted thiophenes were formed and characterized by contact angle measurements, ellipsometry an XPS as well for the SAM of decanethiol, didecylsulfide, thiophene and 3-octylthiophene. Interestingly, the single-chain thiophene derivative forms a thicker SAM than the two-chained derivatives.

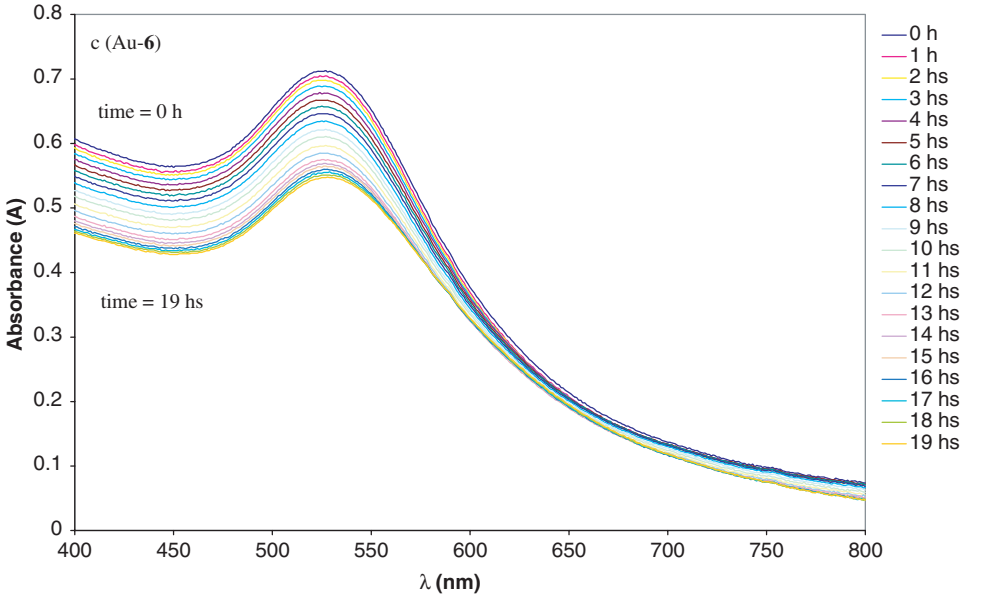

Figure 5. Continued.

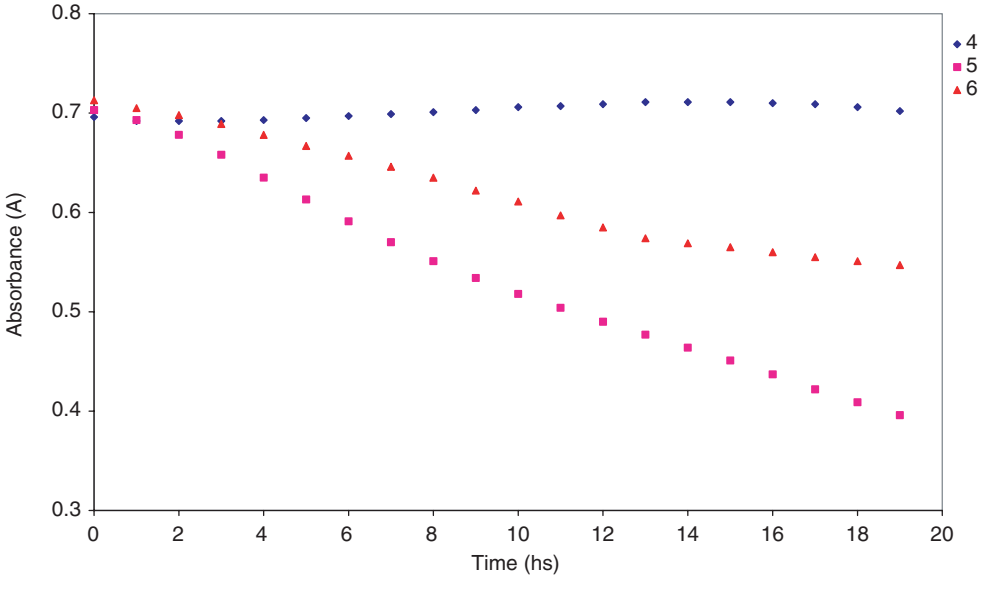

Figure 6. Graph representing the change in the absorbance at λ_{max} for Au nanoparticles passivated with **4**, **5** and **6** over 19 hours.

Au nanoparticles passivated with unsubstituted, 3-monosubstituted and 3,4-disubstituted thiophene derivatives have been synthesized for the first time. Au nanoparticles stabilized with thiophene (**3**) could not be purified due to their lack of stability toward precipitation. The Au nanoparticles passivated with 3-octylthiophene,

3,4-dioctylthiophene and 3,4-diheptyloxythiophene were relatively stable and were characterized by UV/visible spectroscopy, TEM and DLS. As expected TEM revealed the Au nanoparticles stabilized with **4–6** were larger than those stabilized with **1** and **2**. Also as expected the Au nanoparticles stabilized with **4–6** were less stable than the Au nanoparticles stabilized with **1** and **2**. A UV/visible time-dependent spectroscopic study revealed the 3-octylthiophene (**4**) passivated Au nanoparticles were more stable than the 3,4-disubstituted thiophene passivated Au nanoparticles, and the dioctyl (**5**) passivated A-nanoparticles were not as stable as the heptyloxy (**6**) Au nanoparticles. Thus, a delicate interplay between electronics and sterics is controlling the size and stability of the Au nanoparticles stabilized by **4–6**.

Acknowledgements

This work was supported by BAESYSTEMS and EPSRC (DTA to PI). We would like to thank Prof. Graham Leggett for the use of his metal evaporator system.

Appendix

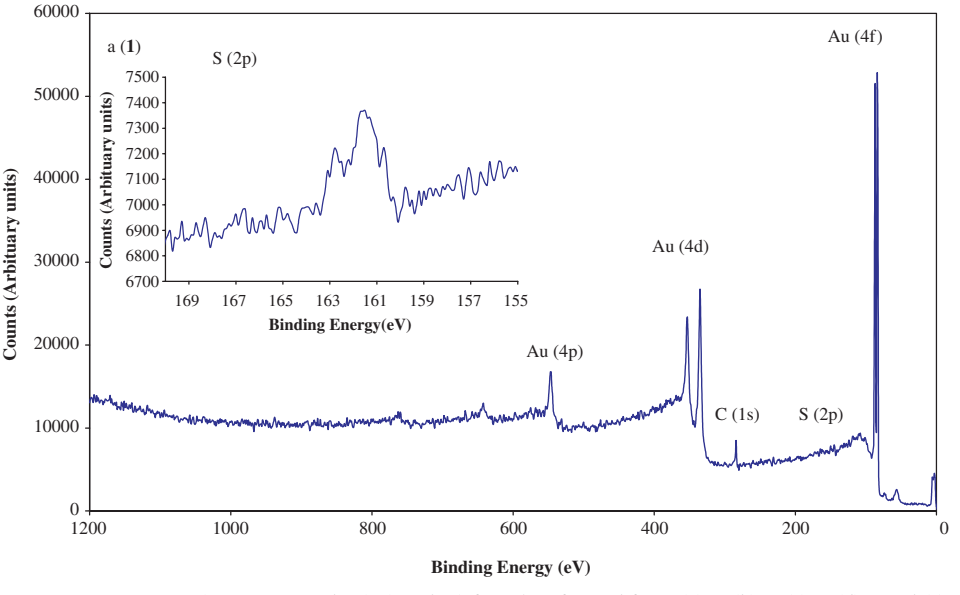

Figure 7. XPS spectra (0–1200 eV and S (2p) region) for SAM formed from (a) **1**, (b) **2**, (c) **3**, (d) **4** and (e) **6**.

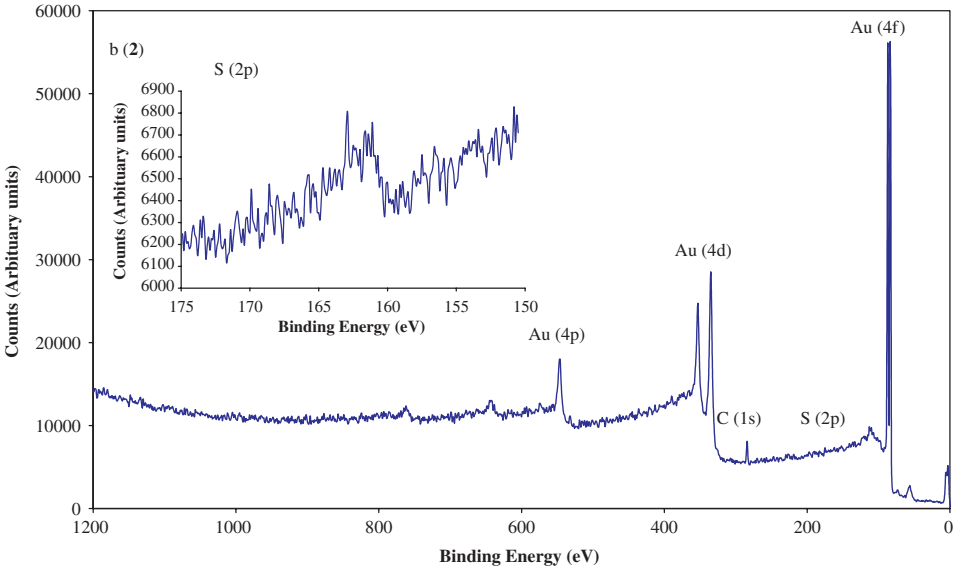

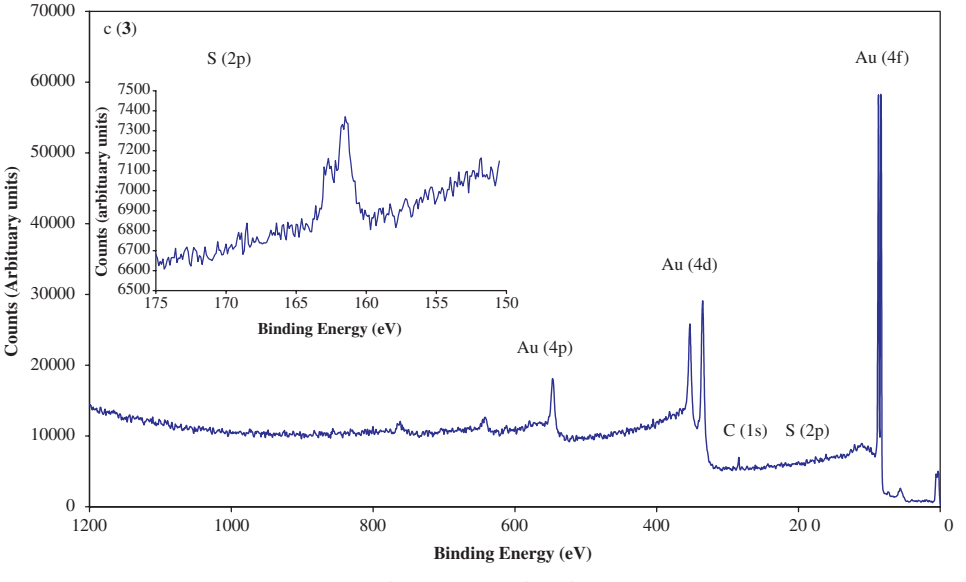

Figure 7. Continued.

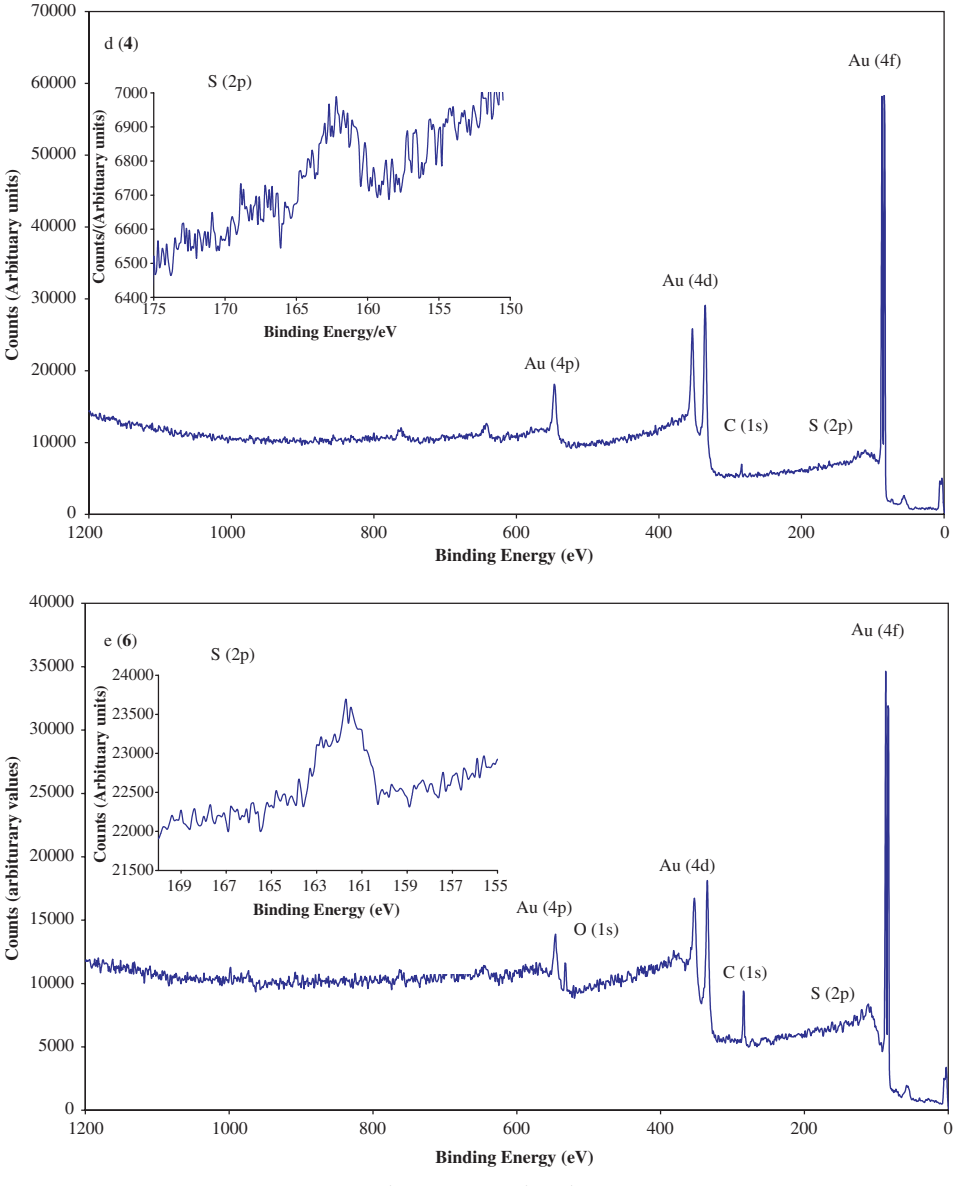

Figure 7. Continued.

References

[1] J.C. Love, L.A. Estroff, J.K. Kriebel, R.G. Nuzzo, G.M. Whitesides. Self-assembled monolayers of thiolates on metals as a form of nanotechnology. *Chem. Rev.*, **105**, 1103 (2005).

[2] U. Weckenmann, S. Mittler, S. Krammer, A.K.A. Aliganga, R.A. Fischer. A study on the selective oragnometallic vapour deposition of palladium onto self-assembled monolayers of 4, 4′-biphenyldithiol, 4-biphenylthiol and 11-mercaptoundecanol on polycrystalline silver. *Chem. Mater.*, **16**, 621 (2004).

[3] L. C. P. M. de Smet, H. Zuilhof, E.J.R. Sudhölter, L.H. Lie, A. Houlton, B.R. Horrocks. Mechanism of the hydrosilylation reaction of alkenes at pourous silicon: experimental and computational deuterium labelling studies. *J. Phys. Chem. B*, **109**, 12020 (2005).
[4] A. Ulman. Formation and structure of Self-Assembled Monolayers. *Chem. Rev.*, **96**, 1533 (1996).
[5] P.E. Laibinis, G.M. Whitesides. Self-assembled monolayers of n-alkanethiolates on copper are barrier films that protect the metal against oxidation by air. *J. Am. Chem. Soc.*, **114**, 9022 (1992).
[6] S. Lee, A. Puck, M. Graupe, R. Colorado Jr, Y.-S. Shon, T.R. Lee, S.S. Perry. Structure, wettability, and frictional properties of phenyl-terminated self-assembled monolayers on gold. *Langmuir*, **17**, 7364 (2001).
[7] X.H. Yang, D.L. Dermody, C. Xu, A.J. Ricco, R.M. Crooks. Molecular interactions between organized, surface-confined monolayers and vapor-phase probe molecules. 8. Reactions between acid-terminated self-assembled monolayers and vapor-phase bases. *Langmuir*, **12**, 726 (1996).
[8] M. Wells, D.L. Dermody, H.C. Yang, T. Kim, A.J. Ricco, R.M. Crooks. Interactions between organized, surface-confined monolayers and vapor-phase probe molecules. 9. Structure/reactivity relationship between three surface-confined isomers of mercaptobenzoic acid and vapor-phase decylamine. *Langmuir*, **12**, 1989 (1996).
[9] Y.-H. La, H.J. Kim, I.S. Maeng, Y.J. Jung, J.W. Park. Differential reactivity of nitro-substituted monolayers to electron beam and x-ray irradiation. *Langmuir*, **18**, 301 (2002).
[10] P. Mendes, M. Belloni, M. Ashworth, C. Hardy, K. Nikitin, D. Filtzmaurice, K. Critchley, S.D. Evans, J.A. Preece. A novel example of x-ray radiation induced chemical reduction of an aromatic nitro-group containing thin film on SiO_2 to an aromatic amine film. *Chem. Phys. Chem.*, **4**, 884 (2003).
[11] R. Haag, M.A. Rampi, R.E. Holmlin, G.M. Whitesides. Electrical breakdown of aliphatic and aromatic self-assembled monolayers used as nanometer-thick organic dielectrics. *J. Am. Chem. Soc.*, **121**, 7895 (1999).
[12] T. Ishida, M. Hara, I. Kojima, S. Tsuneda, N. Nishida, H. Sasaba, W. Knoll. High resolution x-ray photoelectron spectroscopy measurements of octadecanethiol self-assembled monolayers on Au(111). *Langmuir*, **14**, 2092 (1998).
[13] Y.-T. Tao, C.-C. Wu, J.-Y. Eu, W.-L. Lin. Structure evolution of aromatic-derivatized thiol monolayers on evaporated gold. *Langmuir*, **13**, 4018 (1997).
[14] X.M. Yang, R.D. Peters, T.K. Kim, P.F. Nealy. Structure of alkanoic acid stabilized magnetic fluids. A small-angle neutron and light scattering analysis. *Langmuir*, **17**, 228 (2001).
[15] C. Jung, O. Dannenberger, Y. Xu, M. Buck, M. Grunze. Self-assembled monolayers from organosulfur compounds: A comparison between sulfides, disulfides and thiols. *Langmuir*, **14**, 1103 (1998).
[16] M.W.J. Beulen, B.-H. Huisman, P.A. van der Heijden, F. C. J. M. van Veggel, M.G. Simons, E. M. E. F. Biemond, P.J. de Lange, D.N. Reinhoudt. Evidence for nondestructive adsorption of dialkyl sulfides on gold. *Langmuir*, **12**, 6170 (1996).
[17] E.B. Troughton, C.D. Bain, G.M. Whitesides, R.G. Nuzzo, D.L. Allara, M.D. Porter. Monolayer films prepared by the spontaneous self-assembly of symmetrical and unsymmetrical diakyl sulfides from solution onto gold substrates: structures, properties, and reactivity of constituent functional groups. *Langmuir*, **4**, 365 (1998).
[18] T. Matsuura, M. Nakajima, Y. Shimoyama. Growth of self-assembled monolayer of thiophene on gold surface: an infrared spectroscopic study. *Jpn J. Appl. Phys.*, **40**, 6945 (2001).
[19] J. Noh, E. Ito, K. Nakajima, J. Kim, H. Lee, M. Hara. High-resolution STM and XPS studies of thiophene self-assembled monolayers on Au (111). *J. Phys. Chem.*, **106**, 7139 (2002).
[20] J. Noh, K. Kobayashi, H. Lee, M. Hara. Formation kinetics and structure of 3-octylthiophene self-assembled monolayers on gold surfaces. *Chem. Soc. Jpn Chem. Letts*, 601 (2000).
[21] V. Chechik, R.M. Crooks, C.J.M. Stirling. Reactions and reactivity in self-assembled monolayers. *Adv. Mater.*, **12**, 1161 (2000).
[22] F. Schreiber. Self-assembled monolayers: from 'simple' model systems to biofunctionalized interfaces. *J. Phys. Condens. Mater.*, **16**, 881 (2004).
[23] P. Fenter, F. Schreiber, L. Berman, G. Scoles, P. Eisenberger, M.J. Bedzyk. On the structure and evolution of the buried S/Au interface in self-assembled monolayers: x-ray standing wave results. *Surface Chemistry*, **412/413**, 213 (1998).
[24] D.J. Lavrich, S.M. Wetterer, S.L. Bernasek, G. Scales. Physisorption and chemisorption of alkanethiols and alkyl sulfides on Au (111). *J. Phys. Chem. B*, **102**, 3456 (1998).
[25] Qualitative statement made in reference 20.
[26] A. Lachkar, A. Semani, E. Sacher, M. Leclerc, R. Mokhliss. Metallization of polythiophenes I. Interactions of vapour-deposited Cu, Ag and Au with poly(3-hexylthiophene) (P3HT). *Synthetic Metals*, **66**, 209 (1994).
[27] F. Elfeninat, C. Fredriksson, E. Sacher, A. Selmani. A theoretical investigation of the interactions between thiophene and vanadium, chromium, copper, and gold. *J. Chem. Phys.*, **102**, 6153 (1995).

[28] O. Stephan, P. Schottland, P.-Y. Le Gall, C. Chevrot, M. Carrier. Electrochemical behaviour of 3,4-ethylenedioxythiophene functionalised by a sulfonate group. Application to the preparation of poly(3,4-ethylenedioxythiophene) having permanent cation-exchange properties. *J. Electroanal. Chem.*, **443**, 217 (1998).
[29] L. Dodabalapur, L. Torsi, E. Katz. Organic transistors: two dimensional transport and improved electrical characteristics. *Science*, **268**, 270 (1998).
[30] F. Geiger, M. Stolt, H. Schweizer, P. Bäuerle, E. Umbach. Electroluminescence from oligothiophene-based light-emitting devices. *Adv. Mater.*, **5**, 922 (1993).
[31] M. Brust, M. Walker, D. Bethell, D.J. Schiffrin, R. Whyman. Synthesis of thiol derivatised gold nanoparticles in a two-phase liquid-liquid system. *J. Chem. Soc., Chem. Commun.*, 801 (1994).
[32] E.J. Shelley, D. Ryan, S.R. Johnson, M. Couillard, D. Fitzmaurice, P.D. Nellist, Y. Chen, R. E. Palmer, J.A. Preece. Dialkyl sulfides: Novel passivating agents for gold nanoparticles. *Langmuir*, **18**, 1791 (2002).
[33] K. Inoue, S. Shinkai, J. Huskens, D.N. Reinhoudt. Formation of gold colloids using thioether derivatives as stabilising ligands. *J. Mater. Chem.*, **11**, 1919 (2001).
[34] M. Zharnikov, W. Geyer, A. Golzhauser, S. Frey, M. Grunze. Modification of alkanethiolates monolayers on Au substrate by low energy electron irradiation: alkyl chains and the S/Au surface. *Phys. Chem., Chem. Phys.*, **1**, 3163 (1999).
[35] Y. Chen, R.E. Palmer, E.J. Shelly, J.A. Preece. HREELS studies of gold nanoparticles of gold nanoparticles with dialkylsulfide ligands. *Surface Science*, **502–503**, 208 (2002).
[36] C.W. Spangler, M. He. Preparation and oxidative doping studies of dithienyl polyenes stabilised by alkyl group substitution. *J. Chem. Soc. Perkin Trans.*, **1**, 715 (1995).
[37] A.N. Shipway, M. Lahav, R. Gabai, I. Willner. Investiagations into the electrostatically induced aggregation of Au nanoparticles. *Langmuir*, **16**, 8789 (2000).